Journal of Materials and Engineering Structures

Research Paper

Assessment of Influence of Reinforcement Detailing on Blast Resistance of Reinforced Concrete Beam-column Connections

Hafiz Ahmed Waqas [a,*], Ali Husnain [a], Hassan Ubaid [a], Adil Poshad Khan [a], Mati Ullah Shah [a], Muhammad Ilyas [a], Muhammad Waseem [a]

[a] *Department of Civil Engineering, Ghulam Ishaq Khan Institute of Engineering Sciences and Technology, Topi, Swabi, Khyber Pakhtoon khwa, 23640, Pakistan*

ARTICLE INFO

Article history :

Received : 16 Ferbruary 2023

Revised : 23 June 2023

Accepted : 11 July 2023

Keywords:

Beam-column connection

Blast resistance

Damage

Reinforcement detailing

ABSTRACT

This study investigates the influence of blast loading on Reinforced Concrete (RC) beam-column connections, which are critical components for maintaining the structural integrity of buildings during extreme events like explosions. The impact of varying blast loads, detonation distance, and reinforcement detailing on the extent of damage in the RC frame and connections is analyzed using ABAQUS/CAE Finite Element Modelling (FEM) software. Joint rotation is used as a damage indicator to assess the damage level in the structure. The study evaluates the effect of reinforcement detailing on the blast damage resistance of the RC frame and connections and proposes recommendations for reducing damage in the connections through the effective placement of steel reinforcement. The effectiveness of different configurations of reinforcing steel bars is also analyzed, and the presence of shear and diagonal reinforcements is found to reduce joint damage by 3-4 times. This study highlights the significance of reinforcement detailing and recommends its careful consideration in the design of blast-resistant structures.

1 Introduction

RC components are common for the construction of buildings and other infrastructure and are exposed to threats of a variety of impact loadings such as vehicle collisions, bomb explosions, and terrorist attacks throughout their service life [1]. The vulnerability of RC structures under shock and blast loading during numerous terrorist attacks on civil and military infrastructure has risen serious concerns among authorities [2]. These disastrous events have killed several people and have severely damaged the buildings. During the blast event, an enormous amount of energy is released as blast shockwave which travels at supersonic speed and its impact typically lasts between 2 and 20 ms [3-6]. The dynamic response and failure mode under impact and quasistatic loads differ due to the intense energy released in the blast loading over a very brief period of

* *Corresponding author. Tel.: +92313 4010390.*
E-mail address: hafiz.waqas@giki.edu.pk

e-ISSN: 2170-127X,

RESEARCH REVIEW of Sciences and Technologies

time [3]. This catastrophic event can cause both local and global damage to the structure based on the location of blast detonation from the structural components. A near-field detonation of blast will result in transient response of structure through transmission of shockwave and will cause the excessive localized failure and severe damages compared to far-field detonation [4]. Since a large infrastructure and the buildings are the soft target of terrorists, the blast resistant RC structures are essential to prevent immense casualties and loss of property [7].

Restricted data related to structural response under blast loading is available due to security concerns. The majority of blast-resistant design guidelines such as ASCE manual 42, UFC 3-340-01 and UFC 3-340-02 are dedicated for critical infrastructure, like nuclear plants and other defence installations [8, 5, 6]. Limited research has been performed on the blast-resistant behaviour of structures because of the high threat level but short frequency of occurrence. Most nations have not yet established their antiterrorism design codes and these guidelines are mostly restricted to military facilities. For instance, the United States' Department of defence (DoD) deals with such documents for blast resistant design. The recent incidence of bomb explosion on civil infrastructure has brought to light the significance of considering blast load effects on residential and other civil structures against unexpected terrorist attacks and explosive loadings [9]. This situation requires more attention of researchers to establish design guidelines for blast-resistant civil structures.

The blast resistant structures require strong and ductile construction materials with good energy absorption capacity to resist blast pressure and reduce deformations. The reinforced concrete is regarded as an effective structural material to withstand blast loads because of its remarkable capacity to absorb energy and sufficient ductility [5],[10, 11][12]. The residential buildings are typically designed as RC Moment resisting frames (MRF) with monolithic beam-column connections. The integrity of joints plays an important role for providing the performance and safety of RC framed structures. The joint is a critical location of structural system, and its failure can impart serious damage the whole structural system and could initiate the progressive collapse [12][13]. A beam-column joint could fail due to shear mechanism, anchorage failure or bond failure of rebars [14]. The failure of RC member could be controlled by extra reinforcement detailing and the enhanced confinement of the concrete which improves the ductility and offers enhanced energy dissipation against significant inelastic deformations [15].

The external beam-column connections are more vulnerable than internal beam-column connections because of their lesser lateral confinement and reinforcement detailing and anchorage. The performance of exterior beam-column joints was widely investigated considering quasi-static loading in many studies [16-26]. The dynamic response of structure in blast loading is different from quasi-static loading and therefore, these joint needs to be thoroughly investigated for localized blast loads as the weakest link of the structure.

Previous studies investigated the effectiveness of RC members, like beams, slabs, columns, and tunnels subjected to impact and blast loads [27]. Aoude, et al. [28] tested a Steel Fiber Reinforced Column (SFRC) under simulated blast loading conditions to reveal its superior blast-resistant qualities. To describe the response of structures subjected to blast loading, blast simulators like hydraulic blast actuators and shock tubes had been used because of the restrictions on use of explosives. A series of blast simulator tests were performed by Li, et al [29]. on columns that were built with seismic provisions. It was noticed that those columns could offer good ductility and improved damage tolerance as blast resistance. Various design charts including pressure impulse (P-I) diagrams and shock response spectra have been proposed by Krauthammer and Abedini, et al. for forecasting the structural behavior and calculating the damage level in RC structures exposed to blast loading [27]. The design charts were created using an elastic-perfectly plastic resistance function as the basis for a single degree of freedom (SDOF) approximation. The blast overpressures impact on the ductility of an RC member was researched by Krauthammer [27]. The support rotation as performance indicator and ductility were used to evaluate the extent of damage to the structure. It was found that a doubly reinforced beam and column experience severe damage when the member rotation exceeds from the limiting values provided by guidelines [8, 5, 6]. Lim, et al. [9] used finite element method to determine how shear and diagonal reinforcement affected the blast endurance of a beam-column joint and compared the stresses in the reinforcement along with deflection and rotations of RC frame.

According to the review of the literature, the behavior of beam-column joint under blast loading, being most susceptible to such hazards, has received little attention. Most studies concentrate on blast loading away from critical structural location and the impact of blast location on the damage of joint is not fully known. The influence of different reinforcing details on blast-resistant of beam-column joints has been considered but its effects on the damage reduction of the joint is not completely evaluated. Additionally, the extent of damage in RC frame and connection has not been correlated with a damage indicator. Therefore, the performance of a beam-column connection exposed to blast loads is focus of the current research. This

investigation uses numerical methods which have significant advantages over the experimental investigation considering enormous costs and time of repeated blast tests.

The results of this study are expected to enhance the understanding of damage distribution and deformation control of RC beam-column connections subjected to blast loading. The reported results could be utilized for improved blast resistant design of RC beam-column connections. The paper describes the scheme of numerical analysis to simulate the structural response under blast loading in section 2 and discusses the results of the study considering influence of variable distance of blast detonation, amount of explosive charge, and relationship between extent of damage and damage indicator in section 3; and finally, provides the conclusions and recommendations of this study in section 4. The schematic of present study is summarized in Figure 1.

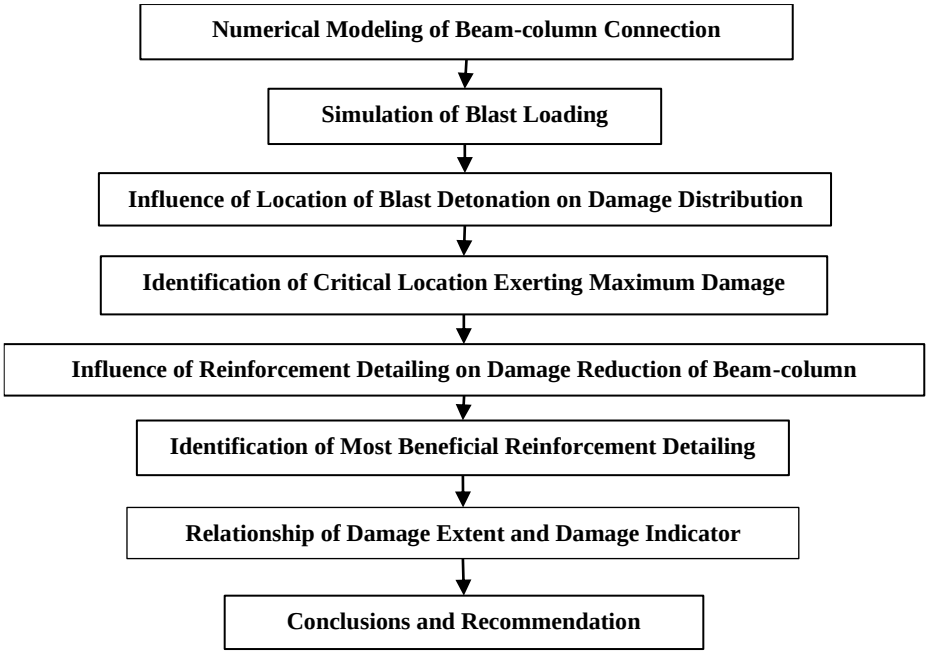

Fig. 1 – Schematic of present study.

2 Numerical modeling scheme

In this research, the impact of blast load is investigated on a numerical model of RC beam-column connection using Abaqus Finite Element Modelling (FEM) [30]. The modelling of material behaviour, geometric details of beam-column connection, and simulation of blast loading are discussed in following sections.

2.1 Material behavior of confined concrete including strain rate effects

The material behaviour of concrete was simulated with Concrete Damage Plasticity (CDP) with strain hardening [31]. The CDP model is plasticity-based a continuum damage model for concrete. It assumes two primary failure mechanisms in the concrete material as compressive crushing and tensile cracking. The CDP utilizes the damage variables d_c and d_t for compression damage and tension damage, respectively. The damage parameters are nondimensional and have maximum value as unity. The value of damage variables ranges between 0 and 1, representing the intact material and complete loss of strength, respectively. The variables increase with the increase in plastic deformation. These damage variables attain a maximum value at any given location in the material and indicate the total damage corresponding to occurrence of a macroscopic crack. These damage parameters are related with inelastic strain based on the plasticity theory. The development of yield surface is regulated by equivalent compressive plastic strain ($\varepsilon_c{}^{pl}$) and equivalent tensile plastic strain ($\varepsilon_t{}^{pl}$), related to failure mechanisms under compression and tension loads. Under uniaxial compression and tension loads, the stress strain relations are provided by the following equations,

$$\sigma_t = (1 - d_t)E_o(\varepsilon_t - {\varepsilon_t}^{pl}) \quad (1)$$

$$\sigma_c = (1 - d_c)E_o(\varepsilon_c - {\varepsilon_c}^{pl}) \quad (2)$$

where E_o is the initial (undamaged) modulus of elasticity of the material and ε_t is total strain.

The biaxial behaviour of concrete material is considered with ratio of equi-biaxial compressive yield stress and uniaxial compressive yield stress ratio (fb_o/fc_o). The CDP model simulates the plastic flow of the material with flow parameters including dilation angle, viscosity, flow potential eccentricity, and coefficient determining the shape of the deviatoric cross-section (K). Table 1 and 2 provide the material properties of concrete and flow parameters of CDP model.

Table 1 - Properties of concrete material.

Properties	Compressive strength, f_c' (MPa)	Tensile strength, f_t (MPa)	Poisson's ratio	Density (Kg/m^3)
Values	45.2	3.2	0.19	2230

Table 2 - Flow parameters of CDP model.

Dilation angle	Eccentricity	fb_o/fc_o	K	Viscosity parameter
40^o	0.1	1.16	0.667	0.1

Under blast loading, capacity of concrete is increased because of impact of transverse confinement and high strain rates [32]. The constitutive model of material requires to include the effects of strain rate and influence of confinement in material behaviour. According to CEB code 2010, ratio of dynamic strength to static strength, known as dynamic increase factor (DIF), could be used in numerical calculations to describe the effects of strain rate on structural materials [33]. The CEB's recommendation for the DIF of concrete's compressive strength is adopted in this study as follows:

$$CDIF = \left(\frac{fcd}{fcs}\right) = \begin{cases} \left[\frac{\dot{\varepsilon}}{\dot{\varepsilon}_s}\right]^{1.026\propto} & , \dot{\varepsilon} \le 30s^{-1} \\ \gamma(\dot{\varepsilon})^{1.3}) & , \dot{\varepsilon} > 30s^{-1} \end{cases} \quad (3)$$

$$\alpha = (5+3fcs/4)^{-1} \quad (4)$$

$$\log\gamma = 6.156\alpha - 0.49 \quad (5)$$

Where, *fcd* represents the dynamic compressive strength for a given strain rate $\dot{\varepsilon}$, *fcs* correspond to static compressive strength and $\dot{\varepsilon}_s = 30 \times 10^{-6}$ s^{-1}.

For concrete tensile strength with strain rate effects, the recommended equations of Malvar and Ross were adopted with strain rate of 1 s^{-1}. The relationship of static and dynamic tensile strength is defined with Tension Dynamic Increase Factor (TDIF) as follow.

$$TDIF = \left(\frac{ftd}{fts}\right) = \begin{cases} \left[\frac{\dot{\varepsilon}}{\dot{\varepsilon}_s}\right]^{\delta}, & \dot{\varepsilon} \le 1s^{-1} \\ \beta(\frac{\dot{\varepsilon}}{\dot{\varepsilon}_s})^{1.3}, & \dot{\varepsilon} > 1s^{-1} \end{cases} \quad (6)$$

$$\log\beta = 6\delta - 2 \quad (7)$$

$$\delta = \left(\frac{1}{1+\frac{8fc}{f_{c0}}}\right) \quad (8)$$

Where *ftd* correspond to dynamic tensile strength for a given strain rate $\dot{\varepsilon}$, *fts* represents static tensile strength, f_{c0} = 10

MPa and $\dot{\varepsilon}_s = 10^{-6} \cdot s^{-1}$. The DIF values of 2 and 6 are adopted for compression and tension, respectively [34, 35].

2.2 Steel constitutive model and strain rate effects

The reinforcing steel was modelled with strain hardening elastic-plastic constitutive behaviour. The CEB code [36] recommended equation was adopted to consider the effects of strain rate for reinforcing steel. For the steel material, the *DIF* is given by

$$DIF = \left(\frac{fyd}{fys}\right) = 1 + \frac{6}{fys} ln\left(\frac{\dot{\varepsilon}}{5\times10^{-5}}\right) \quad (9)$$

Where *fyd* shows the dynamic yield strength for a given strain rate $\dot{\varepsilon}$ and *fys* represents the static yield strength. According to the past experimental work, steel strength under static and dynamic loadings does not differ significantly and DIF could be taken as unity [37]. However, in the present study, the *DIF* of 1.2 was adopted based on the previous work in [9]. The material properties of steel are further provided in Table 3.

Table 3 - Steel material properties.

Properties	Static conditions	Dynamic conditions
Yield strength (MPa)	414	475
Tensile strength (MPa)	620	751
Young's modules (MPa)	2×10^5	2×10^5
Poisson's ratio	0.3	0.3
Density (Kg/m^3)	7869	7869
Elongation (%)	18	35 %

Table 4 - Details of different specimens investigated.

Model	Name	Description
M1	Specimen CB	Code-compliant control specimen
M2	Specimen CB-F	Addition of four No. 36 flexural bars in specimen CB
M3	Specimen CB-D	Addition of four No. 36 diagonal bars in specimen CB
M4	Specimen CB-F-S	Addition of No. 10 shear bars @300 mm in specimen CB-F
M5	Specimen CB-F-S-D	Reinforced with all types of reinforcement specified for flexure, shear, and diagonal bars

2.3 Geometry and model parameters

In this study, the primary aim was to analyze the blast-resistive capacity of RC beam-column connection with various reinforcement detailing. Therefore, five different models with various reinforcement details were created and their geometry was designed in accordance with the requirements of ACI-319 and ACI 352R-19 [38]. The size of column and beam were 560 x 560 mm and 560 x 700 mm, respectively. The length of column and beam were 3700 mm and 1500 mm, respectively [9]. The code compliant control specimen "CB" was designed with the longitudinal steel ratio for reinforced columns as 0.038 Ag (gross area of column cross section), while transverse rebars in column were used as No. 10 ties, and the distance between them was 150 mm. Four No. 36 bars were positioned for the flexural rebar in the beam section. Longitudinal reinforcement in beam was kept continuous through connection without splices. Moreover, the same design approach was used for other specimens and supplementary reinforcement was arranged in each specimen as follows.

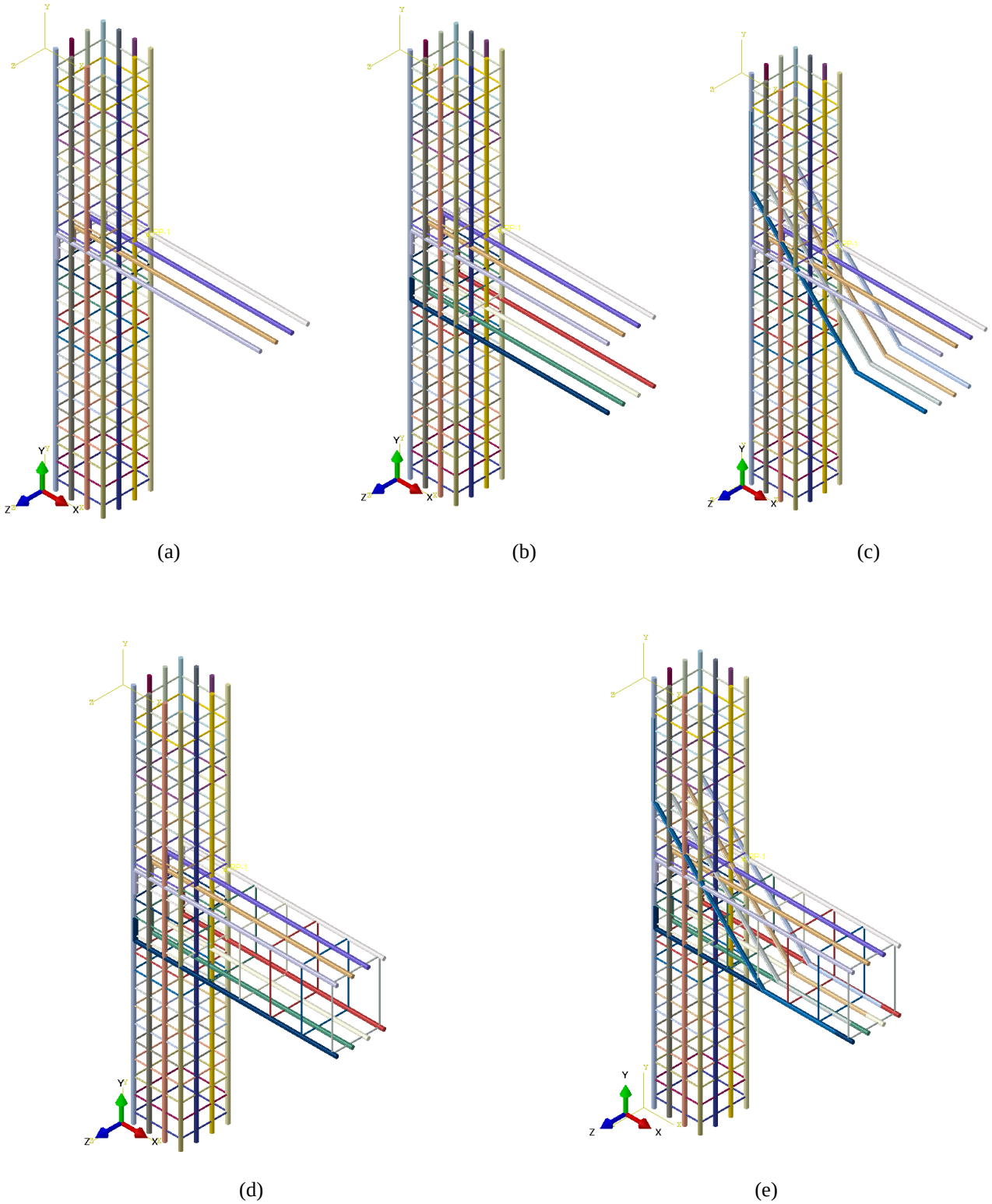

(a) (b) (c)

(d) (e)

Fig. 2 – Overview of different specimens: a) CB, b) CB-F, b) CB-D, d) CB-F-S, e) CB-F-S-D.

The "Specimen CB-F" was also provided with four No. 36 bars at the bottom side of beam to assess the increase in flexural strength and improvement in blast-resistant capacity. Four No. 36 diagonal bars were also added to "Specimen CB-D". With the UFC 3-340-02 as a guide, the diagonal bar's development length was fixed to 720 mm [5]. Design minimum shear

reinforcements were provided in "Specimen CB-F-S" to confirm the effects of shear reinforcement. The "Specimen CB-F-S-D" was provided with all kinds of reinforcement comprising flexural, shear and diagonal bars to exemplify the ambiguous effects of various reinforcements against blast loading. Figure 2 illustrates the five different models developed to examine the effects of blast loads and Table 4 summarizes these all models with different reinforcement detailing schemes used in this study.

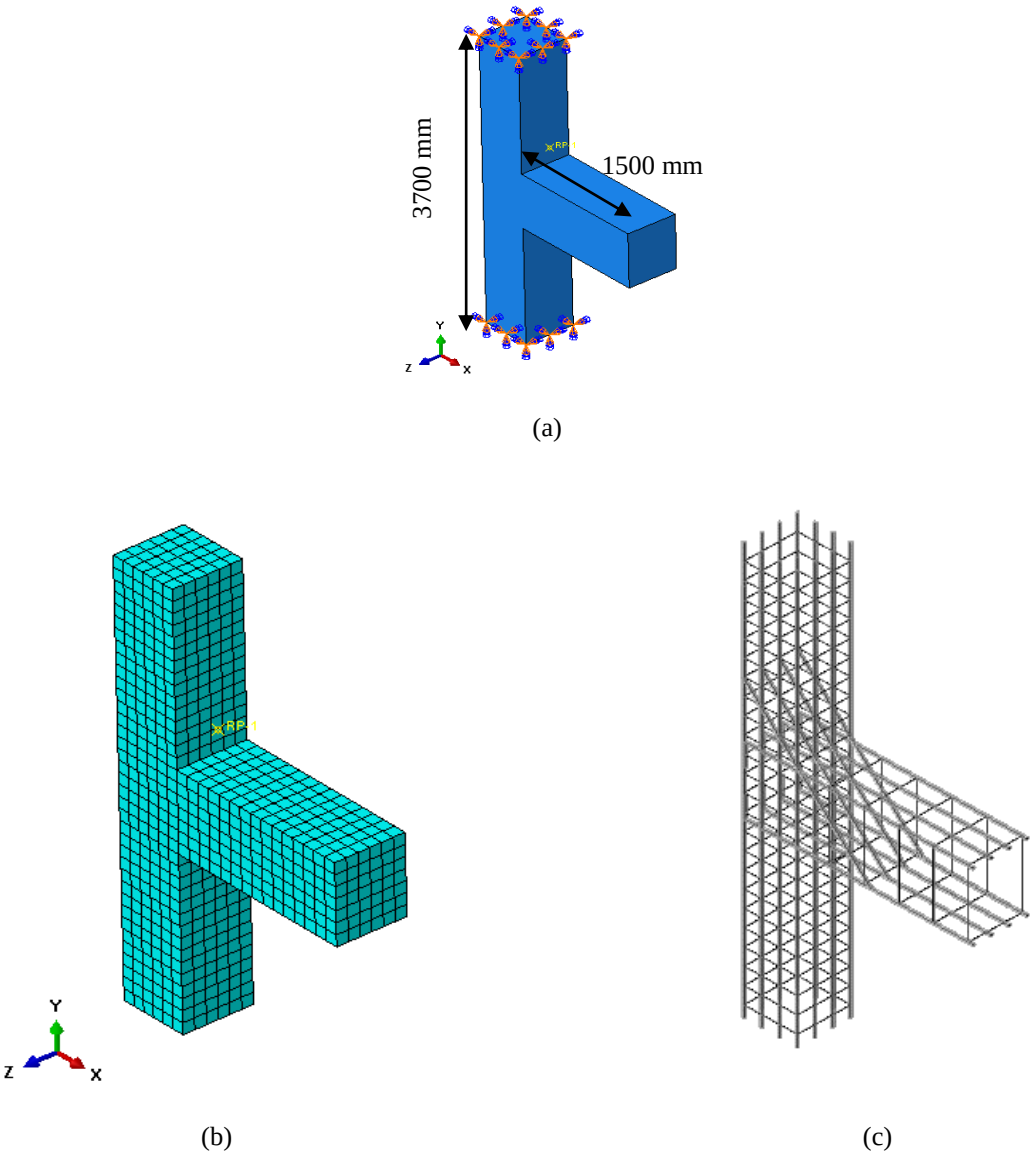

(a)

(b)

(c)

Fig. 3 – Details of FEM of beam-column connection (a) Model geometry with constraints (b) Meshed geometry of concrete (c) Meshed geometry of rebars.

The geometry of the structural components was created as deformable solid body. The interaction of steel and concrete was considered using the embedded region option in Abaqus software wherein the concrete was assumed as host region and the steel was embedded region. The primary objective of this study is to evaluate the maximum deformation and damage occurring at the joint. To achieve this, specific boundary conditions were chosen to induce maximum damage at the joint. Specifically, the free end of the beam and fixed ends of the column were selected as boundary conditions. These particular boundary conditions were selected as they would result in the highest deformation and damage within the joint region by providing appropriate constraints. The rationale behind this choice stems from the previous work conducted by Badrashi et al. [39], where they employed free boundary conditions for the beam to enable unrestricted motion in the vertical direction.

Consistent with their approach, the present study maintains end constraints to impartially investigate the performance of the joint under extreme conditions.

The elements of concrete and steel were discretized for FEM using 3-Dimensional wire elements for reinforcement and 3-Dimensional solid elements for concrete components. The mesh elements for reinforcement were 3-Dimensional, 2 node elements (T3D2). T3D2 elements are used to simulate slender, line-like structures that only enable axial loading along the element and do not support moments or forces that are perpendicular to the centerline. The elements of concrete were meshed with 3-Dimensional, 8 node elements of Reduced integration (C3D8R). C3D8R elements are linear brick elements with fewer integration points and are standard elements for stress analysis. The details of FEM of beam-column connection are shown in Figure 3.

2.4 Simulation of blast loading

Various explosive materials had been used as blast load on the structure as depicted in [40]. This study employed the briefcase category of TNT blast loading as a means to simulate the conditions resulting from an explosion within a building. To ensure numerical solution convergence, a detonation distance of 150 mm between the structural component and the TNT charge was assumed. This selection of detonation distance successfully resolved the convergence difficulty encountered during the numerical analysis. The blast load was incorporated using the interaction module of Abaqus FEM tool. The surface blast load was created using CONWEP blast definition [41]. The main inputs required by CONWEP method are the mass of explosive material and the distance of detonation point. The CONWEP model of Abaqus FEM code converts the mass of explosives to an equivalent amount of TNT. The simulated blast load in the current study was consigned with a reference point at 150 mm height from top surface of the beam and was detonated at specified detonation locations.

2.5 Validation of FEM Modelling

The validation of a numerical model using experimental data is crucial in assessing the reliability and accuracy of the proposed approach. In this study, the proposed FEM modelling approach is validated using experimental data obtained from previous research conducted by Yan et al. [7]. Yan et al.'s research focused on investigating the blast performance of RC beams, where they subjected 10 scaled beam samples to various blast loadings. The properties of the RC beams used in their experiments are summarized in Table 5.

Table 5 - Details of RC beam properties.

Parameter	Values
Dimensions (mm)	150 x 150 x 1700
Compressive Strength (MPa)	30
Longitudinal Bars	4-#8
Stirrups	#6@180
Cover Depth (mm)	20

Table 6 – Peak deflection values compared from experiment and numerical model.

Parameter	Values
TNT Charge (kg)	1
Stand-off Distance (m)	0.5
Peak Deflection Experimental (mm)	99.25
Peak Deflection FEM (mm)	93.8
Percentage Difference (%)	5.5

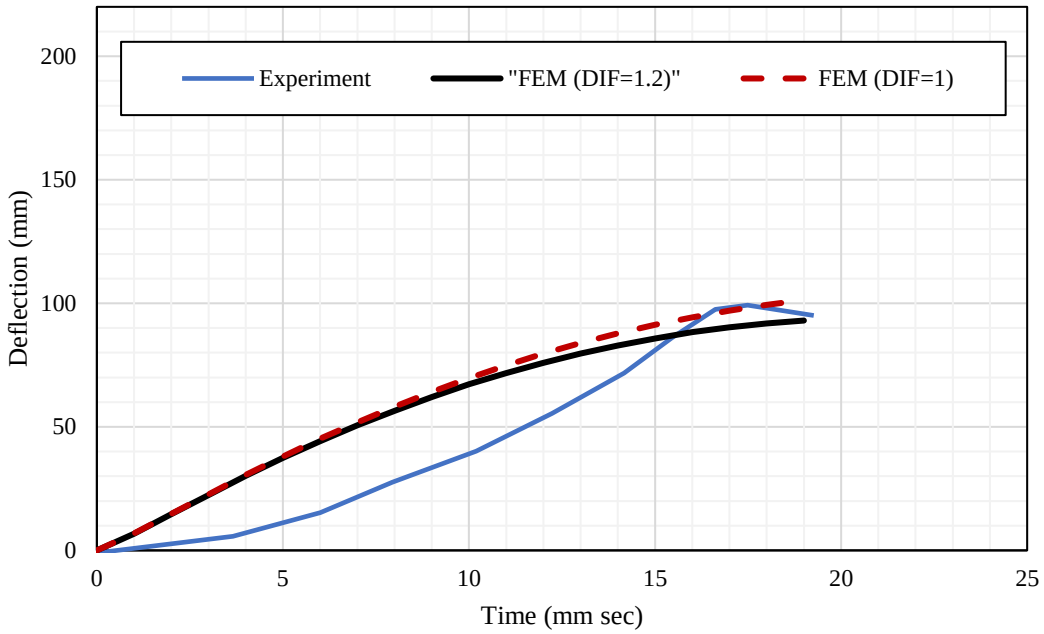

Fig. 4 – Deflection time histories comparison of experimental results and FEM models.

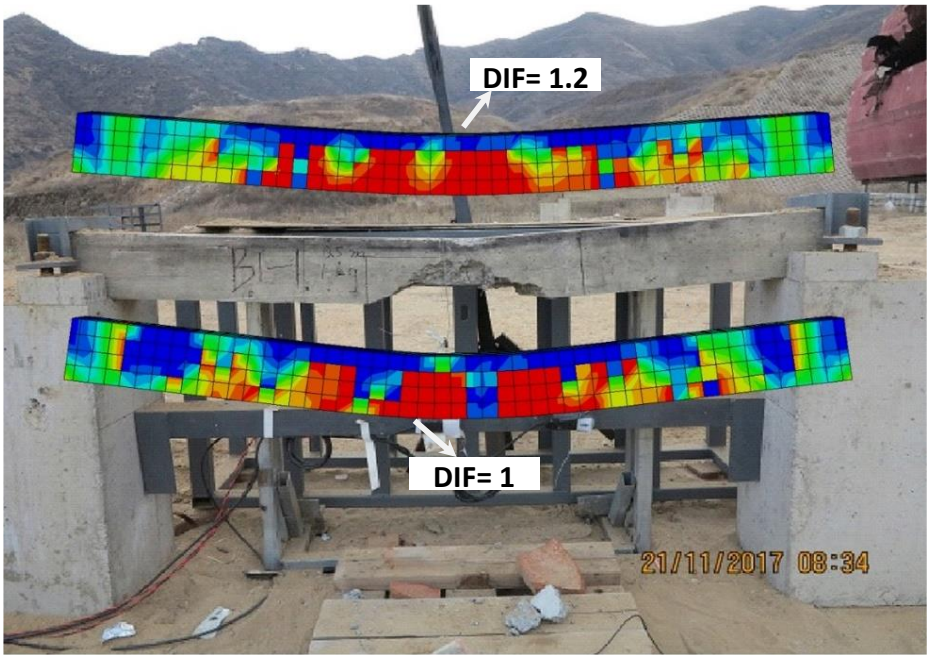

Fig. 5 –Comparison of damage distribution of experimental vs FEM models at different DIF (picture retrieved from [7]).

For validation purposes, a specific experimental model subjected to a 1 kg trinitrotoluene (TNT) charge at a stand-off distance of 0.5 m was chosen. The deflection-time histories obtained from the experimental data of Yan et al. [7] are compared with the results obtained from the FEM models at two different DIF, namely DIF=1 and DIF=1.2, as shown in Figure 4. It is evident that both FEM models exhibit satisfactory agreement with the experimental data near the peak deflection value. However, the FEM model with DIF=1 provides a more accurate prediction of the peak deflection compared to the FEM model with DIF=1.2. Further comparison of the peak deflection values between the experimental data and the numerical model (DIF=1) is presented in Table 6. Moreover, Figure 5 illustrates the distribution of damage within the RC beams for both FEM models, i.e., DIF=1 and DIF=1.2. It can be observed that the FEM model with DIF=1.2 closely resembles the

experimental damage distribution. On the other hand, while the FEM model with DIF=1 accurately represents the peak deflection, a slight discrepancy exists between its damage distribution and the experimental data. It is important to note that the FEM model with DIF=1.2 slightly underestimates the peak deflection value; however, it demonstrates good agreement with the experimental data in terms of damage distribution. These findings underscore the importance of validating the proposed numerical model using experimental data, providing confidence in its reliability and accuracy for further analysis and predictions.

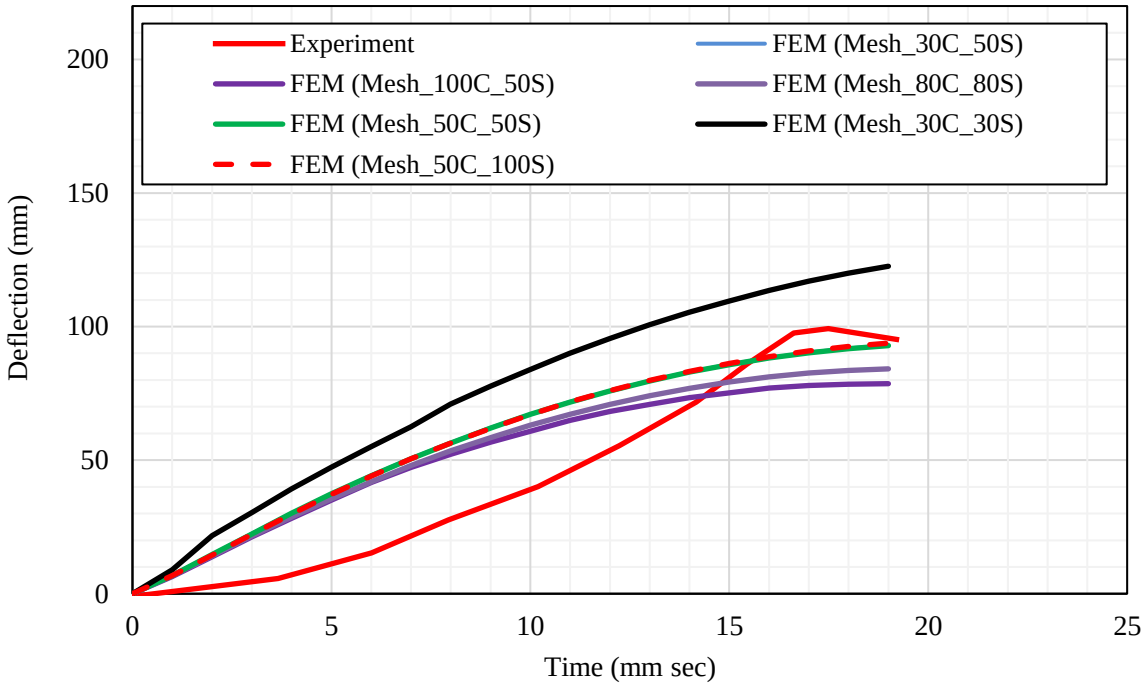

Fig. 6 – Results of Mesh convergence analysis.

2.6 Mesh sensitivity analysis

The numerical models were discretized by selecting appropriate size of the mesh. The initial mesh size was decided by following the results of past research. Foglar and Kovar executed a comparative study of the numerical and experimental analyses involving blast loads . Their study found a good agreement between the experimental and numerical analysis results when mesh size was considered as 30 mm. In this study, therefore, a mesh of 30 element size was initially opted to ensure the reliability of analysis.

The mesh convergence analysis was then carried out by changing the mesh sizes of 100, 80, 50 and 30 mm, for concrete and steel reinforcement. The displacement results of analysis with different mesh sizes and 1 kg mass of TNT blast load, detonated at stand-off distance of 0.5 m were compared with experimental data of RC beam obtained from Yan et al. [7] work. The variation in maximum deflection of numerical model was found to be smaller compared to experimental results when the size of mesh was decreased under 50 mm as shown in Figure 6. Due to the small element sizes, the results were not found to be mesh sensitive; however, the size of the element used in the current study was slightly greater due to a substantially higher element count and longer computation time. In order to achieve an appropriate balance between accuracy and computational efficiency, a mesh size of 50 mm for the concrete elements and 100 mm for the steel reinforcement bar elements (Mesh_50C_100S) was chosen for this study. This mesh configuration resulted in a total of 1962 concrete elements and 1924 steel reinforcement bar elements for the code-compliant control specimen, denoted as "CB". By employing this mesh size, the model can capture the important structural behavior and response while minimizing excessive computational requirements.

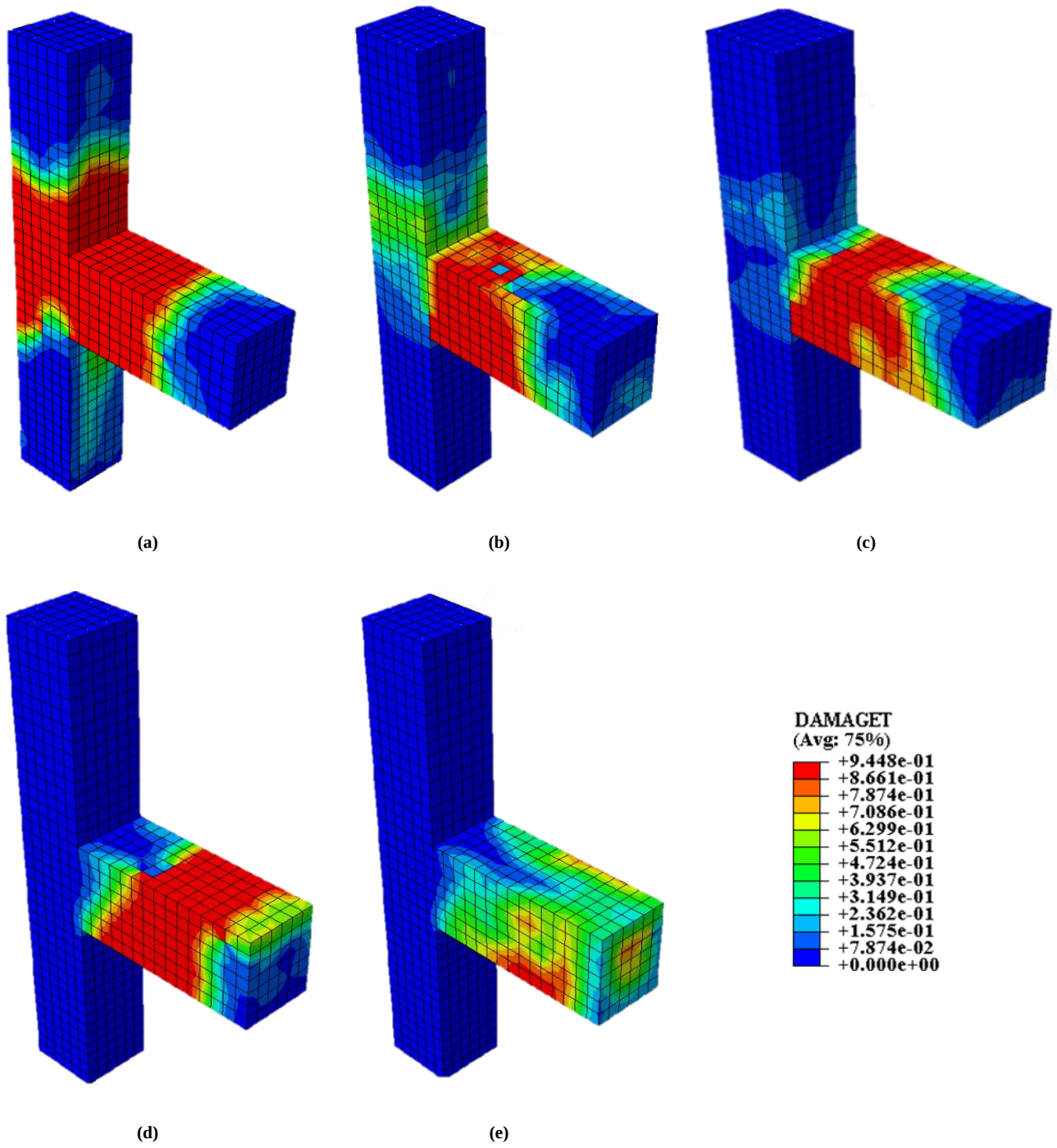

Fig. 7 – Influence of blast location on damage distribution in control specimen: a) 150mm, b) 300mm, c) 600mm, d) 1200mm e) 1500mm.

3 Results and discussion

3.1 Identification of critical blast location

Forces and deformation in the structures subjected to blast loads depend on standoff distance which results in large deformations leading to structural failures. For small standoff distance, blast waves can cause serious damage and failure depends on the location of detonation [42]. The stated scenario was required to be confirmed via numerical implications so the model M4 was used to identify the most crucial blast location which would exert the maximum damage to the beam-

column connection under a given amount of TNT blast. An 8 kg of TNT blast load was placed at different distances from the column face and at a height of 150 mm from the beam surface. The behavior of the target structure under blast loading detonated at different locations was examined and the damage distribution was observed. The structure was subjected to blast load at distances of 150 mm, 300 mm, 600 mm, 1200 mm, and 1500 mm from the column face. Figure 7 exhibits the damage distribution under blast loading detonated at different locations and detonation distance of 150 mm was found to be the most critical one. From the analysis results, it was confirmed that the most critical location of detonation of blast would be closer to the joint which would induce maximum damage and the rotation. The identified location was fixed to further examine the effectiveness of different reinforcement detailing for reducing the damage to structural components under blast loading.

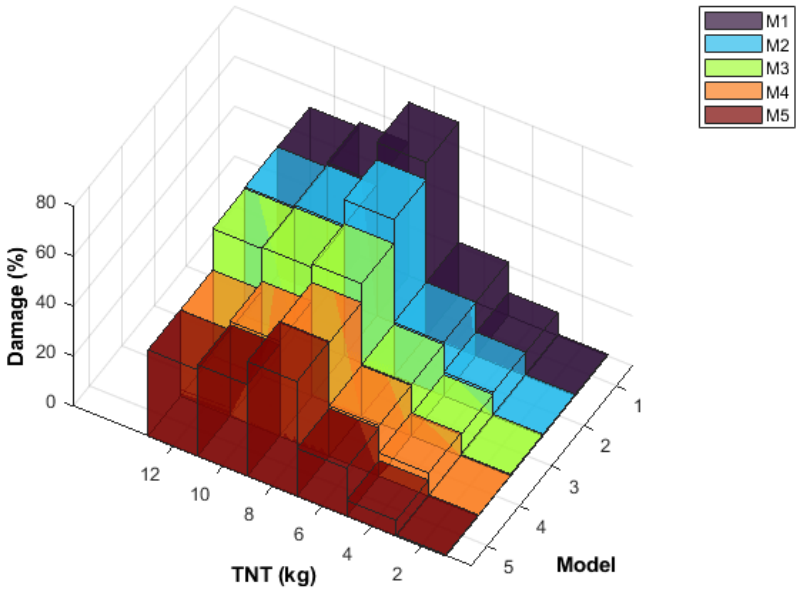

Fig. 8 – Damage vs amount of TNT in different models.

3.2 Influence of different reinforcement detailing

The influence of blast loading on different reinforcement detailing was investigated using different models detailed in Table 4 at critical distance (150 mm). These models were subjected to a range of blast loads from 2 kgs to 12 kgs of TNT. The damage distribution in the specimens was analysed by quantifying the percentage of damage in different components as follows.

$$Damage\ (\%) = \frac{n_{de}}{nt} \times 100 \tag{10}$$

Where, n_{de} is total number of elements experienced more than 50 % damage and n_t is total elements in the model components. The amount of blast damage in these specimens is presented in Figure 8. The models start to suffer from significant damage at 8 kg load of TNT.

From visuals of Figure 8, it can be seen that the damage in the specimen-CB (M1) is maximum. When additional reinforcement was introduced in the structure, damage redistribution and decrease was observed with the increase in amount of reinforcement. In Figure 8, it can be observed that the maximum damage of the specimen occurred when an 8 kg TNT charge was applied. Interestingly, no additional increase in damage was noted with the subsequent increase in the amount of TNT used. This finding suggests that the specimen reached its full capacity following the 8 kg TNT charge, and any further increase in the amount of TNT employed did not result in any additional damage to the specimen. Further, Figure 9 provides additional details of damage distribution in different components of structure under 8 kg of TNT.

When damage in different components was compared it was observed that the beam would endure maximum damage compared to other components. Generally, decrease in damage was observed when additional reinforcement was introduced. For specimen CB-F (M2), which has top and bottom reinforcement in the beam, the damage to connection was reduced significantly and column damage was increased. Further, in the specimen-CB-D (M3), when the diagonal reinforcement was introduced along with top reinforcement in beam, the impact of blast load to column, connection and total structure was reduced from control specimen. In the specimen-CB-F-S (M4), with inclusion of bottom bars and stirrups in beams of control

specimen, the overall damage and damage to other components were decreased. The total damage to structure was also reduced in specimen-CB-F-S-D (M5) by including diagonal reinforcement in specimen M4. The total damage reduction in models M4 and M5 was almost similar however, in model M5, the damage in column and connection was decreased more with the increase in damage to beam. The reinforcement configuration in model M5 induce more damage to beam and promotes the weak-beam strong column concept to control structural damage and prevent complete collapse of structure.

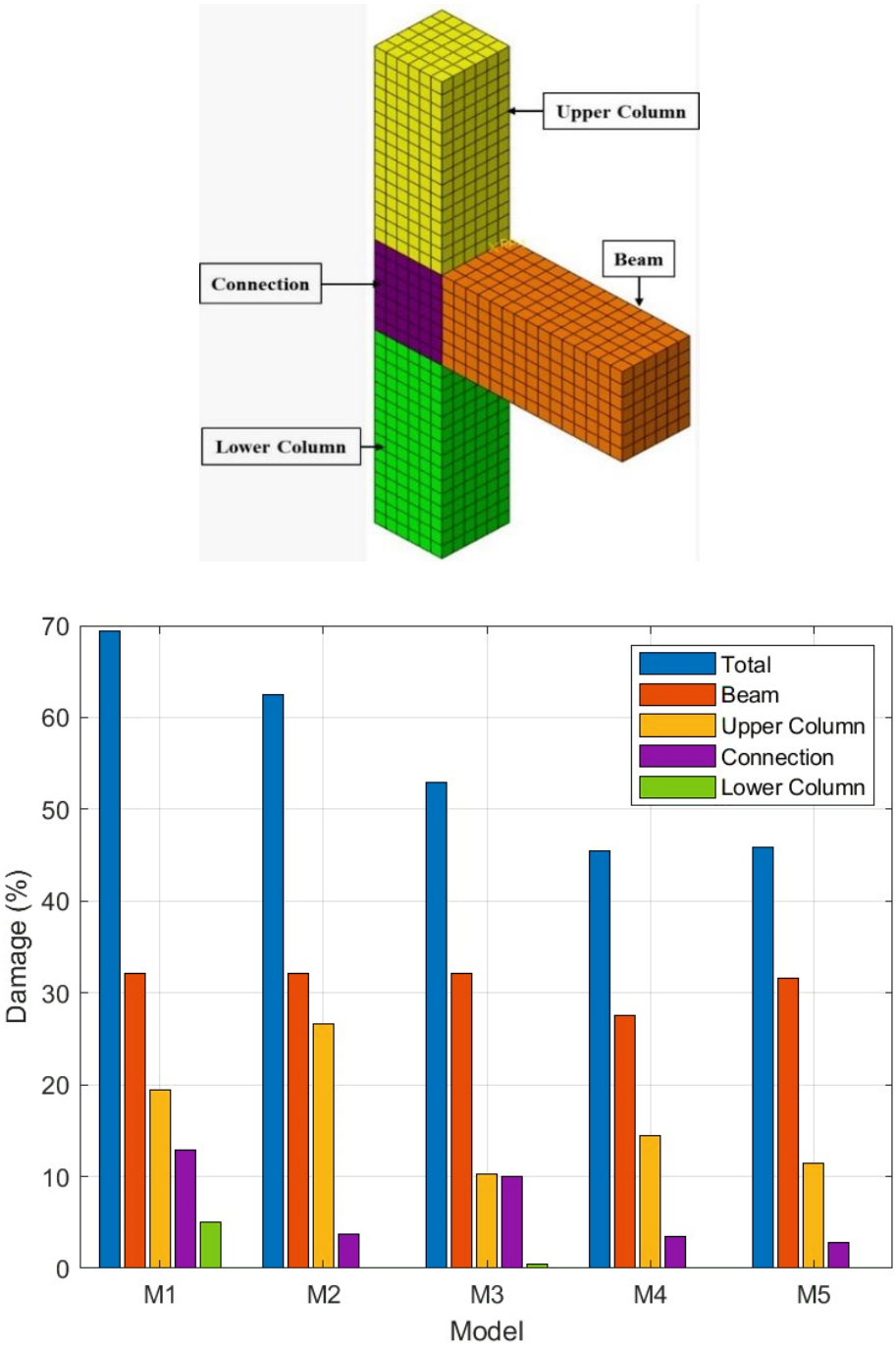

Fig. 9 – Distribution of damage in all models with different reinforcement detailing, under 8 kg of TNT.

The observed changes in the results can be attributed to several plausible causes. The introduction of additional reinforcement in the beam, such as top and bottom reinforcement in model CB-F, diagonal reinforcement in model CB-D, and bottom bars with stirrups in model CB-F-S, led to enhanced load redistribution within the structure. This redistribution mechanism allowed for better stress dissipation and subsequently reduced the overall damage to the components. Moreover,

the inclusion of shear reinforcement, particularly in the form of stirrups, provided improved resistance against shear forces, resulting in a more resilient structure with reduced damage to the column and connection components. The presence of diagonal bars in models CB-D and CB-F-S-D further contributed to the reduction in joint damage by promoting load transfer and enhancing the overall structural performance. The interaction between different reinforcement configurations, including the diagonal bars, played a significant role in enhancing the structural integrity and effectively dissipating blast loads.

The comparison of damage distribution results in all models suggests that specimen-CB-F-S-D (M5) accompany the most effective reinforcement configuration with smallest damage to column, connection, and overall structure. Overall, it is found that the presence of shear and diagonal reinforcements can reduce the joint damage by 3-4 times, respectively. Additionally, the performance of different reinforcement configurations in reducing the joint damage is further evaluated by comparing damage indicator and damage percentage under different amount of blast loads.

3.3 Relationship of damage indicator and damage percentage

The damage indicator and damage percentage of different models were compared for performance evaluation of different reinforcement configurations under various amount of blast loads. The support rotation is the recommended primary criterion of different design guides of blast-resistant structures [5], [8]. As per UFC 3-340-02, maximum joint rotation should be limited to 2 degrees for structural integrity of RC components [5]. The rotation of support was calculated as damage indicator with two different nodes on the upper and lower side of joint. The difference of horizontal deformation at these nodes was divided with height of the beam to get the support rotation. The correlation between joint rotation and damage percentage is shown in Figure 10. From investigation, it was revealed that as mass of the TNT increased, damage and joint rotation were also increased. The control specimen exceeded the 2-degree threshold of joint rotation earlier than other specimens. The joint rotation gradually reduced with introduction of different reinforcements and among all models, the model M5 showed the smallest joint rotation where extreme maximum joint rotation was limited to threshold value of damage indicator.

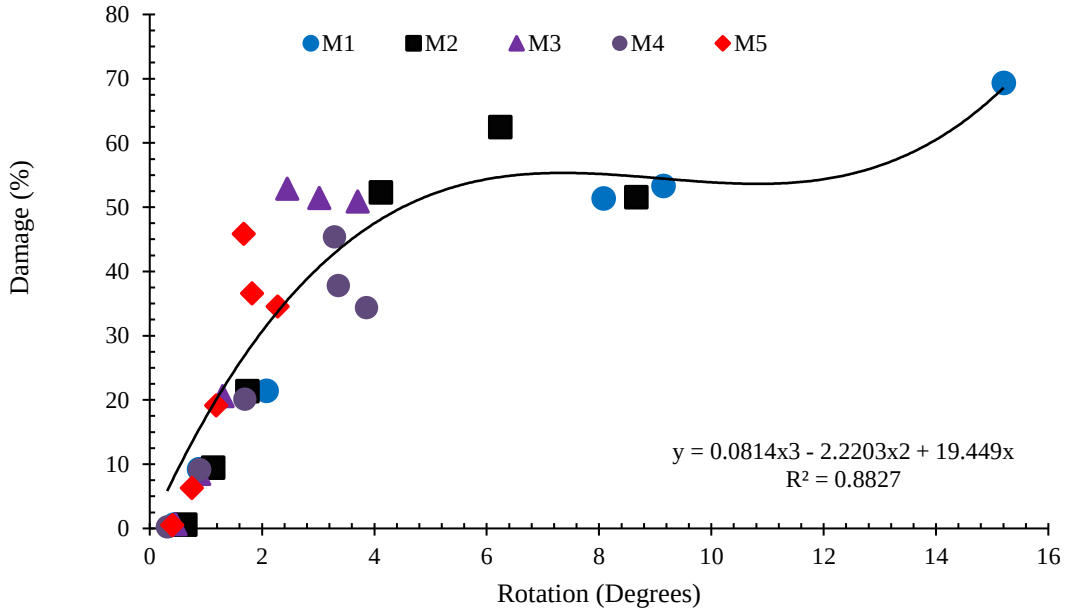

Fig. 10 – Relationship between joint rotation and joint damage.

Figure 11 provides the graphical representation of performance of various reinforcement detailing under different amount of TNT mass in terms of damage percentage and joint rotation. The vertical axis of the Figure 11 is subdivided into two parts where positive axis represents the damage in the structure and negative axis shows the join rotation. The M1 model experienced maximum rotation and damage whereas model M2 got the smaller damage and rotation than M1. The damage and rotation were also reduced in the model M3 by introducing additional diagonal bars. The damage reduction in model M4 was more than model M3 compared to the control specimen M1. Whereas the rotation in model M4 was larger than model

M3. The model M5 suffered least damage and offered minimum joint rotation at ultimate failure. Models M3 and M5 with diagonal reinforcement provided maximum contribution to reduce the joint rotation.

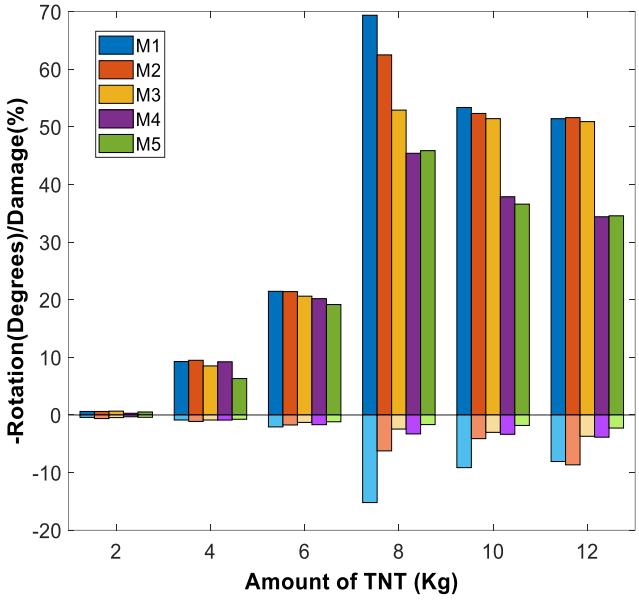

Fig. 11 – Damage percentage and support rotation vs mass of TNT.

The superior performance of the M5 model can be attributed to the combined effects of flexural, diagonal, and shear reinforcement. The presence of flexural reinforcement enabled the model to withstand bending moments, while the diagonal reinforcement strengthened the unity between the column and beam components. Additionally, the inclusion of shear reinforcement enhanced the structure's shear capacity and promoted force redistribution within the joint. These synergistic effects collectively contributed to the minimized joint rotation and reduced damage observed in the M5 model. Thus, the comprehensive reinforcement configuration of M5 demonstrated its effectiveness in enhancing the structural response and mitigating damage in blast-resistant structures.

4 Conclusions and recommendations

This study utilized the FEM analysis approach to investigate the critical blast location exerting maximum damage and evaluate the influence of different reinforcement configurations on blast endurance of RC beam-column connection. The surface blast load of TNT was imposed on the structure to assess the damage propagation at various locations of RC beam-column connection. The blast load at different distances from the joint was first applied to identify the most crucial location which could induce maximum damage to beam-column joint. Next, the identified critical blast location was employed to evaluate the effect of reinforcement detailing on damage distribution and damage reduction in the structure under varying amount of TNT. Following conclusions were drawn from this research.

- The most critical location of detonation of blast was found to be closer to the joint which would induce maximum damage and the joint rotation. The identified location should be considered for impact assessments of blast loading to structural components.

- In comparison to control specimen (M1), the damage redistribution and damage reduction were observed with the introduction of additional reinforcement at different locations of beams.

- The top and bottom bars and stirrups in beams limited the extent of damage to all structural components and whole structure. The presence of shear reinforcements together with flexural bars improved the blast-resistance capability. The blend of shear and flexural reinforcements provided better blast-resistant capabilities due to the confining effects of shear reinforcement.

- Similarly, the combination of top brass, bottom bars, stirrups, and diagonal reinforcement also decreased the overall damage in structural components. However, the larger damage reduction in column and joint was obtained in model M5 and beam suffered more damage than model M4.

- The reinforcement configuration in model M5 induced more damage to beam and would allow beam to fail first than other crucial components of RC frame. This idea is analogous to weak-beam strong column concept to control structural damage and prevent complete collapse of structure and suggests that specimen-CB-F-S-D (M5) accompany the most effective reinforcement configuration with smallest damage to column, connection, and whole structure.

- The comparison of damage indicator and damage percentage under different amount of blast loads in different models revealed that the model M5 offered minimum joint rotation at ultimate failure. Both M3 and M5 models with diagonal reinforcement provided maximum contribution to reduce the joint rotation.

In specimen M5 with all reinforcement types, blast-resistant of structure was appreciably enhanced in terms of better damage distribution and rotation of joint. The effects of combining the flexural, diagonal and shear reinforcements were found greatly beneficial to improve the blast resistance of RC beam-column joints. It was reported that the presence of shear and diagonal reinforcements could reduce the joint damage by 3-4 times, respectively.

Under the extreme blast loadings, the excessive structural damage and joint rotation is expected. Current study investigated the influence of blast load up to the large briefcase category and the required performance of most effective reinforcement configuration under extreme blast loads should also be investigated. Further, the blast resistance of RC beam-column connection with shear heads would be appreciably improved and its performance for enhanced protection against severe blast damages in the structure should be evaluated in the future study.

Acknowledgements

The authors of study would like to thank Department of Civil Engineering of Ghulam Ishaq Khan Institute of Engineering Sciences and Technology Pakistan for providing support in this research.

REFERENCES

[1]- Zhao, W., J. Qian, P. Jia, Peak Response Prediction for RC Beams under Impact Loading. Shock and Vibration. 2019 (2019) 6813693. doi:10.1155/2019/6813693.
[2]- Rajeev, A., S. S. Parsi, S. N. Raman, T. Ngo, A. Shelke, Experimental and numerical investigation of an exterior reinforced concrete beam-column joint subjected to shock loading. International Journal of Impact Engineering. 137 (2020) 103473. doi:10.1016/j.ijimpeng.2019.103473.
[3]- Baker, W. E., P. Cox, J. Kulesz, R. Strehlow, P. Westine, Explosion hazards and evaluation. Elsevier, 2012.
[4]- Meyer, L. W., N. Herzig, F. Pursche, S. Abdel-Malek. Impact Testing and Dynamic Behavior of Materials. New York, NY: Springer New York. 2011.pp. 67-74. doi:10.1007/978-1-4419-9794-4_12.
[5]- USDoD, UFC 3-340-01: Design and Analysis of Hardened Structures to Conventional Weapons Effects, US DoD Washington, DC, USA. (2002).
[6]- USDoD, UFC 3-340-02: Structures to resist the effects of accidental explosions., US DoD Washington, DC, USA. (2008).
[7]- Liu, Y., J.-b. Yan, F.-l. Huang, Behavior of reinforced concrete beams and columns subjected to blast loading. Defence Technology. 14(5) (2018) 550-559. doi:10.1016/j.dt.2018.07.026.
[8]- Dusenberry, D., J. Schmidt, P. Hobelmann, Blast protection of buildings, ASCE/SEI 59-11, Reston: American Society of Civil Engineers. (2011).
[9]- Lim, K.-M., H.-O. Shin, D.-J. Kim, Y.-S. Yoon, J.-H. Lee, Numerical Assessment of Reinforcing Details in Beam-Column Joints on Blast Resistance. International Journal of Concrete Structures and Materials. 10(3) (2016) 87-96. doi:10.1007/s40069-016-0151-x.
[10]- G. M. Verderame, M. T. De Risi, P. Ricci, Experimental Investigation of Exterior Unreinforced Beam-Column Joints with Plain and Deformed Bars. J. Earthq. Eng. 22(3) (2018) 404-434. doi:10.1080/13632469.2016.1233917.
[11]- Ö. Yurdakul , Ö. Avşar, Structural repairing of damaged reinforced concrete beam-column assemblies with CFRPs.

Struct. Eng. Mech. 54(3) (2015) 521–543. doi:10.12989/SEM.2015.54.3.521.
[12]- D. O. Dusenberry, Handbook for blast resistant design of buildings. Hoboken, NJ: Wiley, 2010.
[13]- D. Cormie, G. Mays, P. Smith, Blast effects on buildings. London, UK: Thomas Telford, 2009.
[14]- ACI-ASCE. Recommendations for design of beam-column joints for design of beam column joints in monolithic reinforced concrete structures. Committee 352.1991.
[15]- J. G. MacGregor, J. K. Wight, S. Teng, P. Irawan, Reinforced concrete: Mechanics and design. NJ: Prentice Hall Upper Saddle River, 1997.
[16]- A. Sharma, G. R. Reddy, R. Eligehausen, K. K. Vaze, Strength and ductility of RC beam-column joints of non-safety related structures and recommendations by national standards. Nucl. Eng. Des. 241(5) (2011) 1360–1370. doi:10.1016/j.nucengdes.2011.02.001.
[17]- C. P. Pantelides, J. Hansen, M. J. Ameli, L. D. Reaveley, Seismic performance of reinforced concrete building exterior joints with substandard details. J. Struct. Integr. Maint. 2(1) (2017) 1–11. doi:10.1080/24705314.2017.1280589.
[18]- C. Roehm, S. Sasmal, B. Novák, R. Karusala, Numerical simulation for seismic performance evaluation of fibre reinforced concrete beam-column sub-assemblages. Eng. Struct. 91 (2015) 182–196. doi:10.1016/j.engstruct.2015.02.015.
[19]- J. Nie, Y. Bai, C. S. Cai, New Connection System for Confined Concrete Columns and Beams. I: Experimental Study. J. Struct. Eng. 134(12) (2008) 1787–1799. doi:10.1061/(ASCE)0733-9445(2008)134:12(1787).
[20]- K. Ramanjaneyulu, B. Novák, S. Sasmal, C. Roehm, N. Lakshmanan,N. R. Iyer, Seismic performance evaluation of exterior beam-column sub-assemblages designed according to different codal recommendations. Struct. Infrastruct. Eng. 9(8) (2013) 817–833. doi:10.1080/15732479.2011.625954.
[21]- M. T. De Risi, P. Ricci, G. M. Verderame, Modelling exterior unreinforced beam-column joints in seismic analysis of non-ductile RC frames. Earthq. Eng. Struct. Dyn. 46(6) (2017) 899–923. doi:10.1002/EQE.2835.
[22]- M. T. De Risi, P. Ricci, G. M. Verderame, G. Manfredi, Experimental assessment of unreinforced exterior beam-column joints with deformed bars. Eng. Struct. 112 (2016) 215–232. doi:10.1016/j.engstruct.2016.01.016.
[23]- P. Ricci, M. T. De Risi, G. M. Verderame, G. Manfredi, Experimental tests of unreinforced exterior beam-column joints with plain bars. Eng. Struct. 118 (2016) 178–194. doi:10.1016/j.engstruct.2016.03.033.
[24]- Risi, M. T. D. , G. M. Verderame, Experimental assessment and numerical modelling of exterior non-conforming beam-column joints with plain bars. Eng. Struct. 150 (2017) 115–134. doi:10.1016/j.engstruct.2017.07.039.
[25]- S. Sasmal, B. Novák, K. Ramanjaneyulu, Numerical analysis of fiber composite-steel plate upgraded beam-column sub-assemblages under cyclic lo. Compos. Struct. 93(2) (2011) 599–610. doi:10.1016/j.compstruct.2010.08.019.
[26]- Yurdakul, Ö. , Ö. Avşar, Strengthening of substandard reinforced concrete beam-column joints by external post-tension rods. Eng. Struct. 107 (2016) 9–22. doi:10.1016/j.engstruct.2015.11.004.
[27]- T. Krauthammer, Recent observations on design and analysis of protective structures. Eng. Struct. 149 (2017) 78–90. doi:10.1016/j.engstruct.2016.09.035.
[28]- H. Aoude, F. P. Dagenais, R. P. Burrell, M. Saatcioglu, Behavior of ultra-high performance fiber reinforced concrete columns under blast loading. Int. J. Impact Eng. 80 (2015) 185-202. doi:10.1016/j.ijimpeng.2015.02.006.
[29]- B. Li, A. Nair, Q. Kai, Residual Axial Capacity of Reinforced Concrete Columns with Simulated Blast Damage. J. Perform. Constr. Facil. 26(3) (2012) 287–299. doi:10.1061/(ASCE)CF.1943-5509.0000210.
[30]- D. Systèmes, Abaqus 6.10 online documentation, in Abaqus User Subroutines Reference Manual. (2010).
[31]- J. Lubliner, J. Oliver, S. Oller, E. Oñate, A plastic-damage model for concrete. Int. J. Solids Struct. 25(3) (1989) 299-326. doi:10.1016/0020-7683(89)90050-4.
[32]- J. B. Mander, M. J. N. Priestley, R. Park, Theoretical stress-strain model for confined concrete. J. Struct. Eng. 114(8) (1988) 1804-1826.
[33]- FIB 2010.Fib Model Code for Concrete Structure 2010.2013.
[34]- L. J. Malvar, C. A. Ross, Review of strain rate effects for concrete in tension. ACI Mater. J. 95(6) (1998) 735-739. doi:10.14359/418.
[35]- P.H. Bischoff, S.H. Perry, Compressive behaviour of concrete at high strain rates. Mat. Struct. 24 (1991) 425-450. doi:doi.org/10.1007/BF02472016.
[36]- Comité Euro-International du Béton.Concrete Structures under Impact and Impulsive Loading.1988.
[37]- E. Limberger, K. Brandes, J. Herter. Influence of mechanical properties of reinforcing steel on the ductility of reinforced concrete beams with respect to high strain rates. In: Proceedings of RILEM-CEB-IABSE-IASS

Interassociation Symposium on Concrete Structures under Impact and Impulsive Loading. Berlin, Germany. 1982.pp. 134-156.

[38]- American Concrete Institute-American Society of Civil Engineers (ACI-ASCE) Committee 352, A. R.-.Recommendations for design of beamcolumn connections in monolithic reinforced concrete structures.2019.

[39]- Y.I. Badrashi. Response Modification Factors for Reinforced Concrete Buildings in Pakistan. Ph.D. Thesis. University of Engineering & Technology Peshawar, Pakistan, 2016.

[40]- E. Yandzio, M. Ough, Protection of buildings against explosions, England: Steel Construction Institute London, UK,. (1999).

[41]- D. Hyde, Users' Guide for Microcomputer Programs CONWEP and FUNPRO - Applications of TM 5-885-1, U.S. Army Engineer Waterways Experimental Station Vicksburg, VA. (1988).

[42]- K. Fujikake, B. Li, S. Soeun, Impact response of reinforced concrete beam and its analytical evaluation. J. Struct. Eng. 135(8) (2009) 938-950.